J. Am. Chem. Soc. 1988, 110, 7067-7076 7067

Crown and Extended Organooxotin Compounds Formed with Phosphinate Ligands. A New Class of Tetranuclear Tin Clusters[1,2]

K. C. Kumara Swamy, Charles G. Schmid, Roberta O. Day, and Robert R. Holmes*

Contribution from the Department of Chemistry, University of Massachusetts, Amherst, Massachusetts 01003. *Received February 26, 1988*

Abstract: A new class of organooxotin compounds was discovered by the synthesis of the tetranuclear clusters $[(n\text{-}BuSn)_2OH(O_2PPh_2)_3(OSPPh_2)_2]_2\cdot 8C_6H_6$ (**1**), $[(n\text{-}BuSn(O)O_2P(t\text{-}Bu)_2)(n\text{-}BuSn)(OH)_2O_2P(t\text{-}Bu)_2)]_2[H][O_2P(t\text{-}Bu)_2]$ (**2**), and $[(MeSn(O)O_2P(t\text{-}Bu)_2)(MeSn(OH)(OMe)O_2P(t\text{-}Bu)_2)]_2[H][O_2P(t\text{-}Bu)_2]\cdot 4MeOH\cdot 2H_2O$ (**3**). The former compound **1** has an extended structural array while **2** and **3** have crown structures. All contain hexacoordinated tin atoms with bridging phosphinate ligands and distannoxane linkages. They are synthesized for the most part by reaction schemes employing stannoic and phosphinic acids. ^{119}Sn and ^{31}P NMR characterize their solution-state structures, consistent with their X-ray structures. NMR spectra also show the appearance of a variety of other cluster derivatives arising during synthesis. The Sn-O skeletal arrangement of the crown observed for **2** and **3** is isomeric to the skeletal form of the adamantane structure, the latter of which is present, for example, in $(MeSn)_4S_6$. The occurrence of **1**-**3** suggests the possibility of other oligomeric geometries based on common structural features. **1** crystallizes in the monoclinic space group $P2_1/n$ with a = 17.708 (7) Å, b = 25.884 (10) Å, c = 20.803 (5) Å, β = 110.30 (3)°, and Z = 2. **2** crystallizes in the monoclinic space group $P2_1/n$ with a = 12.658 (4) Å, b = 24.129 (12) Å, c = 26.235 (5) Å, β = 98.03 (2)°, and Z = 4. **3** crystallizes in the orthorhombic space group $Pbcn$ with a = 20.273 (3) Å, b = 16.395 (2) Å, c = 24.320 (4) Å, and Z = 4. The final conventional unweighted residuals are 0.057 (**1**), 0.056 (**2**), and 0.054 (**3**).

Stannoxane clusters containing hexacoordinated tin atoms recently have been found to exist in a variety of new oligomeric forms.[4] These have been characterized as drums[5-8] and ladders,[6,7] cubes,[1b,9] a butterfly,[1b] and oxygen-capped clusters.[1b,10] The number of tin atoms in a particular cluster has ranged from two to six excluding five.

In the previous paper,[1b] tin tetranuclear clusters having a cube as a skeletal structure were reported. For four-coordinated tin, the adamantane structure is known. For example, methyltin sesquisulfide has this geometry.[11] Prior to the X-ray structural determination of this substance, the alternate arrangement of tin-sulfur bridges was considered:[11]

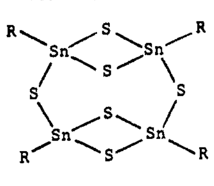

A

In contrast to the admantane structure, which may be viewed as consisting of interlocking six-membered rings, the latter geometry is made up of four- and eight-membered rings. All of the oxo clusters with hexacoordinated tin thus far studied have frameworks consisting of four- and six-membered stannoxane rings. It is possible that phosphinate ligands found effective in forming many of the new tin cluster derivatives might stabilize the skeletal geometry of either the adamantane or alternate A type arrangement.

This paper reports the synthesis of a new class of tetranuclear clusters, $[(n\text{-}BuSn)_2OH(O_2PPh_2)_3(OSPPh_2)_2]_2\cdot 8C_6H_6$ (**1**), $[(n\text{-}BuSn(O)O_2P(t\text{-}Bu)_2)(n\text{-}BuSn(OH)_2O_2P(t\text{-}Bu)_2)]_2[H][O_2P(t\text{-}Bu)_2]$ (**2**), and $[(MeSn(O)O_2P(t\text{-}Bu)_2)(MeSn(OH)(OMe)O_2P(t\text{-}Bu)_2)]_2[H][O_2P(t\text{-}Bu)_2]\cdot 4MeOH\cdot 2H_2O$ (**3**), a determination of their X-ray structures, and a study of their ^{119}Sn and ^{31}P NMR solution-phase spectra. The stannoxane derivative **1** is referred to as an extended cluster while **2** and **3** are termed crown clusters.

Experimental Section

Chemicals were obtained from Aldrich, Fisher Scientific, and Alfa and used without further purification. Methylstannoic acid was prepared according to the procedure given by Lambourne.[12] Di-*tert*-butylphosphinic acid was prepared by literature methods.[13] *n*-Butylstannoic acid was a gift from Koriyama Kasei Co., Ltd., and was purified by using excess KOH in $CHCl_3$ to remove a small amount of $n\text{-}BuSn(OH)Cl_2$ and/or $n\text{-}BuSn(OH)_2Cl$ suspected[7] as a contaminant. Solvents used were of HPLC grade (Fisher Scientific). Further purification was done according to standard procedures.[14]

^1H, ^{31}P, and ^{119}Sn NMR spectra (proton decoupled) were recorded on a Varian XL 300 FT/NMR spectrometer equipped with a multinuclear broad-band probe and operated at 300, 121.4, and 111.862 MHz, respectively. Resonances are referenced vs tetramethylsilane (^1H), tetramethyltin (external standard, ^{119}Sn), and 85% orthophosphoric acid (external standard, ^{31}P). Infrared spectra were recorded by using KBr windows on a Perkin-Elmer Model 180 spectrometer.

Preparation of Diphenylthiophosphinic Acid, $Ph_2P(S)OH$. Diphenylchlorophosphine (11 g, 50 mmol) was stirred with water (25 mL) for 20 min at 25 °C. A suspension of sulfur in toluene (20 mL) was added, and the mixture was stirred overnight during which time a solid remained; mp 128-132 °C. Recrystallization from toluene gave a solid, mp 138-140 °C (lit. mp 143 °C[15]) (yield 3.0 g, 26%). ^{31}P NMR

---

[1] (a) Organotin Clusters. 5. (b) Holmes, R. R.; Kumara Swamy, K. C.; Schmid, C. G.; Day, R. O. *J. Am. Chem. Soc.* companion paper in this issue.

[2] Holmes, R. R.; Day, R. O.; Kumara Swamy, K. C.; Schmid, C. G.; Chandrasekhar, V.; Holmes, J. M. *Abstracts of Papers*, 195th National Meeting of the American Chemical Society, Toronto, Canada, June 1988; American Chemical Society: Washington, DC, 1988; Abstract INOR 346.

[3] This work represents in part a portion of the Ph.D. Thesis of C.G.S., University of Massachusetts, Amherst, MA.

[4] Holmes, R. R.; Day, R. O.; Chandrasekhar, V.; Schmid, C. G.; Holmes, J. M. *Abstracts of Papers*, 193rd National Meeting of the American Chemical Society, Denver, CO, April 1987; American Chemical Society: Washington, DC, 1987; Abstract INOR 385.

[5] Chandrasekhar, V.; Day, R. O.; Holmes, R. R. *Inorg. Chem.* **1985**, *24*, 1970-1971.

[6] Holmes, R. R.; Schmid, C. G.; Chandrasekhar, V.; Day, R. O.; Holmes, J. M. *J. Am. Chem. Soc.* **1987**, *109*, 1408-1414.

[7] Chandrasekhar, V.; Schmid, C. G.; Burton, S. D.; Holmes, J. M.; Day, R. O.; Holmes, R. R. *Inorg. Chem.* **1987**, *26*, 1050-1056.

[8] Day, R. O.; Chandrasekhar, V.; Kumara Swamy, K. C.; Holmes, J. M.; Burton, S. D.; Holmes, R. R. *Inorg. Chem.* **1988**, *27*, 2887-2893.

[9] Kumara Swamy, K. C.; Day, R. O.; Holmes, R. R. *J. Am. Chem. Soc.* **1987**, *109*, 5546-5548.

[10] Day, R. O.; Holmes, J. M.; Chandrasekhar, V.; Holmes, R. R. *J. Am. Chem. Soc.* **1987**, *109*, 940-941.

[11] von Kobelt, D.; Paulus, E. F.; Scherer, H. *Acta Crystallogr., Sect., B: Struct. Crystallogr. Cryst. Chem.* **1972**, *B28*, 2323-2326.

[12] Lambourne, H. *J. Chem. Soc.* **1922**, *121*(2), 2533-2540.

[13] Mason, G. W.; Lewey, S. *J. Inorg. Nucl. Chem.* **1974**, *36*, 911-915.

[14] Vogel, A. I. *Textbook of Practical Organic Chemistry*; Longman: London, 1978.

0002-7863/88/1510-7067$01.50/0

($CDCl_3$; ppm): 74.0.[16] Anal. Calcd for $C_{12}H_{11}OPS$: C, 61.54; H, 4.70. Found: C, 61.75; H, 4.73.

Preparation of the Extended Cluster $[(n\text{-}BuSn)_2OH(O_2PPh_2)_3(OSPPh_2)_2]_2\cdot 8C_6H_6$ (1). A mixture of *n*-butylstannoic acid (1.09 g, 5.24 mmol) and diphenylthiophosphinic acid (1.23 g, 5.24 mmol) were heated together in toluene (75 mL) for 4 h. A Dean–Stark apparatus was used for the azeotropic removal of water. The solvent was evaporated under vacuum, and diethyl ether was added to the residue. A solid **4** remained after filtration. The mother liquor was evaporated to dryness and redissolved in a dichloromethane/benzene mixture (30 mL + 15 mL). Slow evaporation of the solvent over a period of time (~7 days) gave **1** as clear square type crystals, mp >300 °C (yield 0.15 g, 3.2% based on stannoic acid). ^{119}Sn NMR ($CDCl_3$ + MeOH; ppm): −544.0 (minor m), −575.0 (major m), and −614.0 (major, m). ^{31}P NMR ($CDCl_3$ + MeOH; ppm): complex with four groups of signals in the regions 20–30 (two sets, Ph_2PO_2 groups) and 60–80 (two sets, $Ph_2P(O)S$ groups). Anal. Calcd for $C_{148}H_{150}O_{18}P_{10}S_4Sn_4$: C, 56.78; H, 4.80. Found: C, 57.14; H, 5.03. This analysis corresponds to **1**, which has lost six molecules of benzene.

Solid product **4** (yield 0.87 g, 40%) shows a complex broad ^{119}Sn NMR ($CDCl_3$) signal, possibly a doublet, at −465 ppm. Anal. Calcd for $C_{64}H_{76}O_8S_4P_4Sn_4$: C, 45.22; H, 4.47. Found: C, 45.36; H, 4.53. This analysis corresponds to a cube formulation, $[n\text{-}BuSn(O)SOP(Ph)_2]_4$.

Preparation of the Crown Cluster $[(n\text{-}BuSn(O)O_2P(t\text{-}Bu)_2)(n\text{-}BuSn(OH)_2O_2P(t\text{-}Bu)_2)]_2[H][O_2P(t\text{-}Bu)_2]$ (2). *n*-Butylstannoic acid (0.56 g, 2.7 mmol) was dissolved in benzene (125 mL). Heating with stirring was begun while di-*tert*-butylphosphinic acid (0.96 g, 5.4 mmol) was added. The clear solution present was refluxed for $3^1/_4$ h. A Dean–Stark trap was used to azeotropically remove water. Subsequent rotary evaporation yielded a white solid. Dissolution of this solid in a mixture of benzene (2 mL), methylene chloride (2 mL), and ether (2 mL) gave large parallelepiped crystals (0.22 g) identified as di-*tert*-butylphosphinic acid. Filtration and evaporation of the filtrate to dryness gave a crystalline mass. A ^{119}Sn NMR spectrum was recorded (Figure 7b). Redissolution of the crystalline mass in a mixture of methanol (3 mL), chloroform (3 mL), and ether (3 mL) and evaporation gave a similar crystalline mass. Another ^{119}Sn NMR was taken (Figure 7c). After addition of toluene (5 mL) and methanol (0.5 mL) to the crystalline mass, crystals of **2** were obtained (Figure 7d); mp 340 °C (yield 0.2 g, 20%). ^{119}Sn NMR ($CDCl_3$; ppm): −535.3 (dd, ^2J(Sn–O–P) 145, 181 Hz). ^{31}P NMR ($CDCl_3$; ppm): +58.56 (s, with $^{119/117}Sn$ satellites, 143.8, 137.4 Hz), +58.54 (s, with $^{119/117}Sn$ satellites, 190.2, 182.4 Hz), +50.7 (s, $(t\text{-}Bu)_2PO_2^-$). Anal. Calcd for $C_{56}H_{129}O_{16}P_5S_4$: C, 39.82; H, 7.71. Found: C, 40.01; H, 7.90. A crystal from this final product was used for the X-ray study.

Additional synthetic attempts led to detection of **2** in solution by NMR but did not result in isolation of the pure material in Reaction Schemes A and B. However, a small yield of pure crystalline **2** was obtained from Reaction Scheme C.

Reaction Scheme A. *n*-Butylstannoic acid (0.14 g, 0.66 mmol) and di-*tert*-butylphosphinic acid (0.14 g, 0.79 mmol) were dissolved in equiportions (30 mL each) of methanol and toluene. This solution was heated with stirring for 1 h. Rotary evaporation left a viscous liquid. The entire reaction product was dissolved in $CDCl_3$, and ^{119}Sn and ^{31}P NMR spectra were recorded. On the basis of integration of the ^{119}Sn peaks, a yield of the crown **2** of approximately 10% is indicated. ^{119}Sn NMR ($CDCl_3$; ppm) (Figure 7a): −474.9 (t, ^2J(Sn–O–P) = 127.1 Hz), −512.7 (t, ^2J(Sn–O–P) = 151 Hz), −525.5 (dd, ^2J(Sn–O–P) = 139, 204 Hz), −530.4 (t, ^2J(Sn–O–P) = 143 Hz), −535.5 (dd, ^2J(Sn–O–P) = 144, 191 Hz). ^{31}P NMR ($CDCl_3$; ppm): 64.6 (s, with $^{119/117}Sn$ satellites, 138 Hz), 62.8 (s, br), 62.1 (s, with $^{119/117}Sn$ satellites, 127 Hz), 58.7 (s, probably two singlets overlapping with two sets of $^{119/117}Sn$ satellites, 139, 188 Hz), 54.7 (s, with $^{119/117}Sn$ satellites, 194, 204 Hz).

Reaction Scheme B. To a solution of *n*-butyltin trichloride (1.6 g, 5.5 mmol) in dry chloroform (125 mL) was added silver di-*tert*-butylphosphinate (4.7 g, 19.0 mmol) under an atmosphere of dry nitrogen. The contents were heated under reflux for 3 h and filtered. Acetonitrile (50 mL) was added to the filtrate upon which a white solid appeared. This solid, after filtration, was dissolved in diethyl ether (25 mL), and the insoluble material was filtered off. Evaporation afforded a crystalline mass, which on dissolving in tetrachloromethane (15 mL) and standing overnight gave solid di-*tert*-butylphosphinic acid (~1 g). After filtration and evaporation, the filtrate yielded a white solid (~1 g). On the basis of the estimated integration of the ^{119}Sn NMR spectrum, **2** is present in approximately 20% yield. NMR spectra were recorded on a sample of the solid dissolved in $CDCl_3$. ^{119}Sn NMR ($CDCl_3$; ppm): −474.9 (t, ^2J(Sn–O–P) = 128 Hz), −512.2 (t, ^2J(Sn–O–P) = 159 Hz), −523.7 (dd, ^2J(Sn–O–P) = 140, 201 Hz), −535.2 (dd, ^2J(Sn–O–P) = 145, 195 Hz). ^{31}P NMR ($CDCl_3$; ppm): 64.6 (s), 62.8 (s, br), 62.2 (s, with $^{119/117}Sn$ satellites, 121 Hz), 58.7 (s, probably two singlets overlapping with two sets of $^{119/117}Sn$ satellites, 140, 194 Hz), 54.8 (s).

Reaction Scheme C. A mixture of hexameric *n*-butyloxotin acetate, $[n\text{-}BuSn(O)O_2CCH_3]_6$ (0.44 g, 1.8 mmol), and di-*tert*-butylphosphinic acid (0.32 g, 1.8 mmol) was dissolved in toluene (60 mL). This solution was stirred at 25 °C for 15 h and then refluxed for 6 h. Rotary evaporation gave a white solid. Crystallization from a chloroform solution gave **2** (0.060 g, 8% yield). NMR spectra refer to the initial white solid product. ^{119}Sn NMR ($CDCl_3$; ppm): −491.2 (d, ^2J(Sn–O–P) = 132 Hz), −535.5 (dd, ^2J(Sn–O–P) = 146, 192 Hz), −541.4 (d, ^2J(Sn–O–P) = 140 Hz), −556.7 (dd, ^2J(Sn–O–P) = 141, 204 Hz), −560.9 (dd, ^2J(Sn–O–P) = 143, 175 Hz). ^{31}P NMR ($CDCl_3$; ppm): 65.4 (s), 64.4 (s, br), 63.8 (s), 62.0 (s, with $^{119/117}Sn$ satellites, 129 Hz), 60.9 (s), 59.0 (s, br), 56.0 (s).

Preparation of the Crown Cluster $[(MeSn(O)O_2P(t\text{-}Bu)_2)(MeSn(OH)(OMe)O_2P(t\text{-}Bu)_2)]_2[H][O_2P(t\text{-}Bu)_2]\cdot 4MeOH\cdot 2H_2O$ (3). A mixture of the mixed-drum derivative $[(MeSn(O)O_2CMe)(MeSn(O)O_2P(t\text{-}Bu)_2)]_3$ (**5**) (0.135 g, 0.083 mmol), prepared as described previously,[8] and di-*tert*-butylphosphinic acid (0.045 g, 0.25 mmol) was heated together in a chloroform (15 mL)/water (3 mL) heterophase system at 60 °C to dryness on a water bath. This process was repeated three times followed by three successive treatments using a chloroform (15 mL)/water (3 mL)/methanol (5 mL) mixture. More phosphinic acid (0.012 g, 0.07 mmol) was added, and the evaporation process was repeated three more times at 60 °C in a chloroform/water/methanol mixture. Finally, the residue was washed with water (5 mL) to remove residual phosphinic acid (Figure 9a) and was dissolved in a dichloromethane (5 mL)/methanol (20 mL) mixture. A small amount (~0.03 g) of a crystalline material was separated at this stage (Figure 9b). Slow evaporation of the solvent at room temperature afforded **3** in the form of large crystals, mp >380 °C (yield 0.13 g, 70%). ^{119}Sn NMR ($CDCl_3$ + MeOH; ppm): −515.4 (dd, ^2J(Sn–O–P) = 139, 181 Hz). ^{31}P NMR ($CDCl_3$ + MeOH; ppm): 60.7 (s, with $^{119/117}Sn$ satellites, ~171 Hz), 59.6 (s, with $^{119/117}Sn$ satellites, ~133 Hz), 50.2 (s, $(t\text{-}Bu)_2PO_2^-$). Anal. Calcd for $C_{50}H_{131}O_{22}P_5Sn_4$: C, 35.05; H, 7.65. Found: C, 33.87; H, 7.08. The low values may result from the presence of a small amount of a cube derivative or loss of some methanol of crystallization.

X-ray Studies. All X-ray crystallographic studies were done with an Enraf-Nonius CAD4 diffractometer and graphite-monochromated molybdenum radiation (λ(Mo K$\bar{\alpha}$) = 0.710 73 Å) at an ambient temperature of 23 ± 2 °C. Details of the experimental procedures have been described previously.[17]

Crystals were mounted in thin-walled glass capillaries, which were sealed as a precaution against moisture sensitivity for **2** and in order to maintain the integrity of the crystals for **1** and **3**. Data were collected by the θ–2θ scan mode with $3° \le 2\theta_{Mo\,K\bar{\alpha}} \le 43°$.

The structures were solved by use of Patterson and difference Fourier techniques and were refined by full-matrix least squares.[18]

All computations were performed on a Microvax II computer using the Enraf-Nonius SDP system of programs.

X-ray Study for $[(n\text{-}BuSn)_2OH(O_2PPh_2)_3(OSPPh_2)_2]_2\cdot 8C_6H_6$ (1). Crystals of **1** are colorless polyfaceted chunks, which degrade immediately upon removal from the mother liquor. The crystal used for the X-ray study was wedged into a thin-walled glass capillary tube in the presence of a small amount of mother liquor and was approximately square pyramidal with maximum dimensions of 0.50 × 0.63 × 0.63 mm.

Crystal Data: $C_{136}H_{138}O_{18}S_4P_{10}Sn_4\cdot 8C_6H_6$, monoclinic space group $P2_1/n$ (alternate setting of $P2_1/c\text{-}C_{2h}^5$ (No. 14)[19]), a = 17.708 (7) Å, b = 25.884 (10) Å, c = 20.803 (5) Å, β = 110.30 (3)°, Z = 2, $\mu_{Mo\,K\bar{\alpha}}$ = 0.74 mm^{-1}. A total of 10 201 independent relfections ($+h,+k,\pm l$) was measured. An empirical absorption correction based on ψ scans was applied (relative transmission factors from 0.94 to 1.00 on I).

The 80 independent carbon atoms comprising the pendant atoms of the butyl and phenyl groups and the benzene of solvation were poorly defined, and these were included in the refinement as isotropic scatterers. Two positions were found for atom C3 of the butyl group bonded to Sn1 (C3A and C3B, half-occupancy). The remaining 30 independent nonhydrogen atoms were refined anisotropically. Hydrogen atoms were

---

(15) Higgins, W. A.; Vogel, P. W.; Craig, W. G. *J. Am. Chem. Soc.* **1955**, *77*, 1864–1866.

(16) A ^{31}P NMR signal at 34.0 ppm was assigned to Ph_2PO_2H. It represented less than 2% of the total.

(17) Sau, A. C.; Day, R. O.; Holmes, R. R. *Inorg. Chem.* **1981**, *20*, 3076–3081.

(18) The function minimized was $\sum w(|F_o| - |F_c|)^2$, where $w^{1/2} = 2F_oLp/\sigma_I$. Mean atomic scattering factors were taken from: Reference 19, 1974; Vol. IV, pp 72–98. Real and imaginary dispersion corrections were taken from the same source, pp 149–150.

(19) *International Tables for X-ray Crystallography*; Kynoch: Birmingham, England, 1969; Vol. I, p 99.

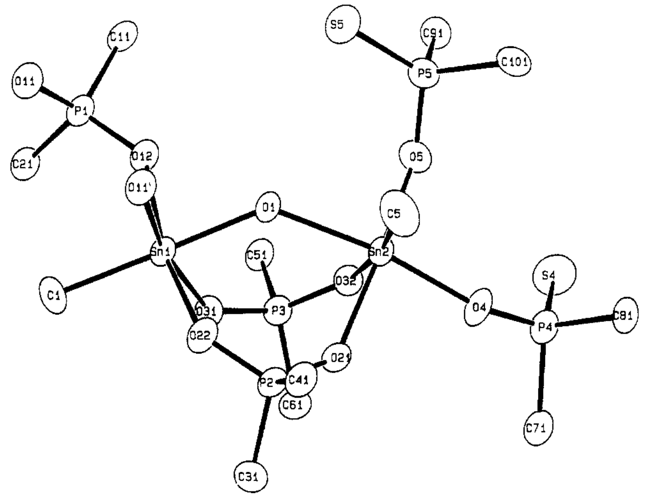

Figure 1. ORTEP plot of the asymmetric unit for $[(n\text{-BuSn})_2OH(O_2PPh_2)_3(OSPPh_2)_2]_2 \cdot 8C_6H_6$ (**1**) with thermal ellipsoids at the 30% probability level. The symmetry-related O11′ (−*x*, −*y*, −*z*) is included to complete the coordination sphere of Sn1. Pendant carbon atoms of the *n*-Bu and Ph groups and all atoms of the benzene of solvation are omitted for purposes of clarity. Phenyl group carbon atoms are labeled C11–C16, C21–C26, etc. *n*-Butyl group carbon atoms are labeled C1–C4 and C5–C8.

omitted from the refinement. The final agreement factors[20] were $R = 0.057$ and $R_w = 0.080$ for the 8039 reflections having $I \geq 3\sigma_I$.

X-ray Study for $[(n\text{-BuSn(O)}O_2P(t\text{-Bu})_2)(n\text{-BuSn(OH)}_2O_2P(t\text{-Bu})_2)]_2[H][O_2P(t\text{-Bu})_2]$ (2). The colorless crystal used for the X-ray study was cut from a cluster of lath-shaped crystals and had an irregular wedge shape with maximum dimensions of 0.33 × 0.38 × 0.40 mm.

Crystal Data: $C_{56}H_{131}O_{16}P_5Sn_4$, monoclinic space group $P2_1/n$, $a = 12.658$ (4) Å, $b = 24.129$ (12) Å, $c = 26.235$ (5) Å, $\beta = 98.03$ (2)°, $Z = 4$, $\mu_{\text{Mo K}\bar{\alpha}} = 1.40$ mm^{-1}. A total of 9081 independent reflections ($+h,+k,\pm l$) was measured. An empirical absorption correction based on ψ scans was applied (relative transmission factors from 0.93 to 1.00 on I).

The 42 independent carbon atoms comprising the pendant atoms of the normal and *tert*-butyl groups were poorly defined, and these were included in the refinement as isotropic scatterers. The remaining 39 independent non-hydrogen atoms were refined anisotropically. Hydrogen atoms were omitted from the refinement. The final agreement factors[20] were $R = 0.056$ and $R_w = 0.079$ for the 6809 reflections having $I \geq 2\sigma_I$.

X-ray Study for $[(\text{MeSn(O)}O_2P(t\text{-Bu})_2)(\text{MeSn(OH)(OMe)}O_2P(t\text{-Bu})_2)]_2[H][O_2P(t\text{-Bu})_2] \cdot 4MeOH \cdot 2H_2O$ (3). Colorless, chunky, polyfaceted crystals of **3** lose solvent slowly when removed from the mother liquor and left in an open container. The crystal used for the X-ray study, cut from a larger crystal, had dimensions of 0.31 × 0.38 × 0.44 mm and degraded only slightly during data collection.

Crystal Data: $C_{46}H_{111}O_{16}P_5Sn_4 \cdot 4CH_3OH \cdot 2H_2O$, orthorhombic space group $Pbcn\text{-}D_{2h}^{14}$ (No. 60),[21] $a = 20.273$ (3) Å, $b = 16.395$ (2) Å, $c = 24.320$ (4) Å, $Z = 4$, $\mu_{\text{Mo K}\bar{\alpha}} = 1.38$ mm^{-1}. A total of 4655 independent reflections ($+h,+k,+l$) was measured. A linear decay correction was applied (correction factors from 1.000 to 1.068 on I). No corrections were made for absorption.

Of the 41 independent non-hydrogen atoms, 38 were refined anisotropically. The three independent non-hydrogen atoms comprising the loosely bound methanol and water of solvation were poorly defined, but their persistent reappearance on difference Fourier syntheses and their sensible geometry with respect to hydrogen bonding and unoccupied space in the cell prompted us to include them in the refinement as isotropic scatterers. Hydrogen atoms were omitted from the refinement. The final agreement factors[20] were $R = 0.054$ and $R_w = 0.079$ for the 3296 reflections having $I \geq 3\sigma_I$.

Results

The atom-labeling scheme and the molecular geometry for **1** are shown in Figures 1 and 2. Atomic coordinates are given in Table I while selected bond distances and angles are given in Table II. The corresponding information for **2** and **3** is given in Figures 2–4 and in Tables III–VI. Anisotropic thermal parameters and additional bond lengths and angles for all three substances are provided as supplementary material.

All three substances represent new structural forms for tin comprising an extended cluster, **1**, and two crown clusters, **2** and **3**. All are relatively thermally stable substances, melting at >300 °C (**1**), at 340 °C (**2**), and >380 °C (**3**). Outside of the loss of

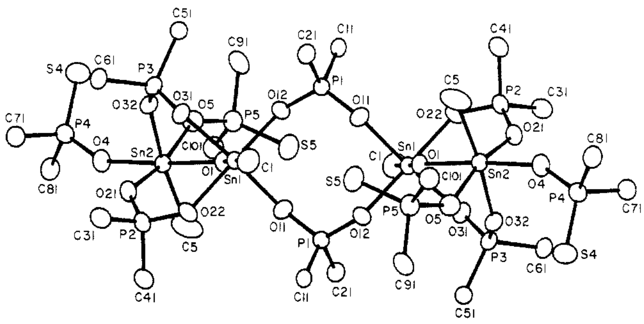

Figure 2. ORTEP plot of the $[(n\text{-BuSn})_2OH(O_2PPh_2)_3(OSPPh_2)_2]_2$ molecule in **1** with thermal ellipsoids at the 30% probability level. Atoms with the same label are related by a crystallographic inversion center (−*x*, −*y*, −*z*).

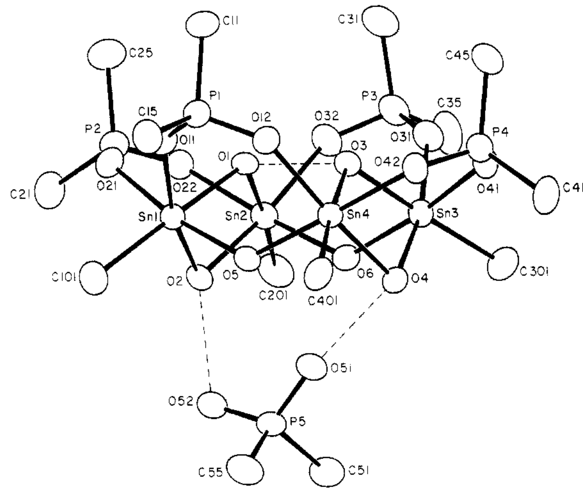

Figure 3. ORTEP plot of $[(n\text{-BuSn(O)}O_2P(t\text{-Bu})_2)(n\text{-BuSn(OH)}_2O_2P(t\text{-Bu})_2)]_2[H][O_2P(t\text{-Bu})_2]$ (**2**) with thermal ellipsoids at the 30% probability level. Pendant carbon atoms of the butyl groups are omitted for purposes of clarity. Hydrogen-bonding interactions are indicated by dashed lines. Carbon atoms of the *n*-Bu groups are labeled C101–C104, C201–C204, etc. Carbon atoms of the *t*-Bu groups are labeled C11–C14, C15–C18, C21–C24, etc.

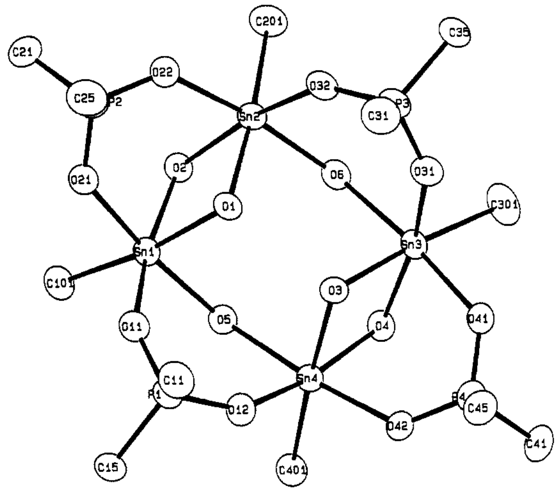

Figure 4. ORTEP plot of the $[(n\text{-BuSn(O)}O_2P(t\text{-Bu})_2)(n\text{-BuSn(OH)}_2O_2P(t\text{-Bu})_2)]_2$ moiety in **2** viewed down the pseudo 2-fold axis. Thermal ellipsoids are at the 30% probability level. Pendant carbon atoms are omitted for purposes of clarity.

---

(20) $R = \sum||F_o| - |F_c||/\sum|F_o|$ and $R_w = \{\sum w(|F_o| - |F_c|)^2/\sum w|F_o|^2\}^{1/2}$.
(21) Reference 19, p 149.

Table I. Atomic Coordinates in Crystalline $[(n\text{-BuSn})_2OH(O_2PPh_2)_3(OSPPh_2)_2]_2 \cdot 8C_6H_6$ (**1**)[a]

atom[b]	x	y	z	B_{eq}[c]
Sn1	−0.06654 (3)	0.03005 (2)	0.08641 (2)	3.32 (1)
Sn2	−0.08466 (3)	−0.05922 (2)	0.23308 (2)	3.36 (1)
S4	−0.2757 (2)	−0.1338 (1)	0.2809 (1)	6.79 (7)
S5	−0.0075 (1)	−0.1675 (1)	0.1237 (1)	6.25 (6)
P1	−0.1245 (1)	−0.02444 (9)	−0.07236 (9)	3.66 (5)
P2	−0.0279 (1)	0.06551 (9)	0.2499 (1)	4.15 (5)
P3	−0.2379 (1)	0.00111 (9)	0.1196 (1)	3.64 (5)
P4	−0.1901 (1)	−0.09126 (9)	0.3403 (1)	4.27 (5)
P5	−0.0850 (1)	−0.17964 (9)	0.1704 (1)	4.46 (5)
O1	−0.0556 (3)	−0.0367 (2)	0.1428 (2)	3.7 (1)
O4	−0.1260 (3)	−0.0699 (2)	0.3125 (2)	5.2 (1)
O5	−0.1214 (3)	−0.1314 (2)	0.1912 (3)	4.7 (1)
O11	−0.0517 (3)	−0.0134 (2)	−0.0920 (3)	4.6 (1)
O12	−0.1103 (3)	−0.0222 (2)	0.0036 (2)	4.0 (1)
O21	−0.0786 (3)	0.0205 (2)	0.2591 (2)	4.2 (1)
O22	−0.0167 (3)	0.0675 (2)	0.1808 (2)	4.8 (1)
O31	−0.1811 (3)	0.0347 (2)	0.0972 (2)	4.0 (1)
O32	−0.1990 (3)	−0.0406 (2)	0.1721 (2)	3.8 (1)
C1	−0.0731 (5)	0.0988 (3)	0.0284 (4)	5.3 (2)
C2	−0.1443 (9)	0.1336 (7)	0.0211 (8)	12.2 (5)*
C3A[d]	−0.142 (2)	0.187 (1)	−0.001 (2)	11.6 (9)*
C3B[d]	−0.141 (1)	0.160 (1)	0.069 (1)	8.2 (6)*
C4	−0.210 (1)	0.211 (1)	0.041 (1)	20.1 (9)*
C5	0.0417 (7)	−0.0761 (4)	0.2849 (5)	7.6 (3)
C6	0.0658 (8)	−0.0964 (6)	0.3494 (7)	10.5 (4)*
C7	0.1692 (9)	−0.1050 (7)	0.3817 (8)	12.3 (5)*
C8	0.177 (1)	−0.1510 (8)	0.358 (1)	15.2 (6)*
C11	−0.1641 (4)	−0.0880 (3)	−0.0989 (3)	3.9 (2)
C12	−0.2173 (5)	−0.0963 (4)	−0.1648 (4)	5.3 (2)*
C13	−0.2468 (6)	−0.1478 (4)	−0.1858 (5)	6.8 (2)*
C14	−0.2216 (6)	−0.1875 (4)	−0.1395 (5)	7.1 (3)*
C15	−0.1695 (6)	−0.1791 (4)	−0.0720 (5)	7.2 (3)*
C16	−0.1393 (5)	−0.1281 (4)	−0.0519 (4)	5.6 (2)*
C21	−0.1996 (4)	0.0213 (3)	−0.1180 (4)	4.1 (2)
C22	−0.1841 (6)	0.0522 (5)	−0.1665 (5)	7.4 (3)*
C23	−0.2422 (8)	0.0900 (6)	−0.2002 (7)	10.0 (4)*
C24	−0.3169 (8)	0.0930 (5)	−0.1866 (7)	9.5 (3)*
C25	−0.3292 (7)	0.0615 (5)	−0.1379 (6)	8.0 (3)*
C26	−0.2706 (5)	0.0246 (4)	−0.1046 (4)	5.4 (2)*
C31	−0.0755 (5)	0.1239 (3)	0.2615 (4)	4.7 (2)
C32	−0.1367 (5)	0.1231 (4)	0.2889 (5)	6.0 (2)*
C33	−0.1743 (6)	0.1715 (5)	0.2963 (5)	7.4 (3)*
C34	−0.1481 (7)	0.2168 (5)	0.2768 (6)	8.7 (3)*
C35	−0.0868 (8)	0.2168 (5)	0.2516 (7)	9.5 (3)*
C36	−0.0475 (6)	0.1701 (5)	0.2433 (5)	7.7 (3)*
C41	0.0704 (5)	0.0621 (4)	0.3142 (4)	4.9 (2)
C42	0.0804 (5)	0.0551 (4)	0.3823 (5)	5.7 (2)*
C43	0.1573 (7)	0.0493 (3)	0.4320 (6)	8.0 (3)*
C44	0.2238 (7)	0.0537 (5)	0.4136 (6)	8.6 (3)*
C45	0.2157 (8)	0.0600 (5)	0.3434 (7)	9.7 (4)*
C46	0.1364 (6)	0.0639 (4)	0.2927 (5)	7.4 (3)*
C51	−0.3069 (4)	−0.0306 (3)	0.0458 (4)	3.8 (2)
C52	−0.2849 (5)	−0.0783 (4)	0.0264 (4)	5.1 (2)*
C53	−0.3360 (6)	−0.1017 (4)	−0.0354 (5)	6.4 (2)*
C54	−0.4080 (6)	−0.0778 (4)	−0.0742 (5)	6.5 (2)*
C55	−0.4299 (6)	−0.0310 (4)	−0.0542 (5)	6.1 (2)*
C56	−0.3794 (5)	−0.0066 (4)	0.0062 (4)	5.0 (2)*
C61	−0.2950 (4)	0.0430 (3)	0.1546 (4)	4.2 (2)
C62	−0.3304 (5)	0.0216 (4)	0.1987 (4)	5.3 (2)*
C63	−0.3762 (6)	0.0572 (4)	0.2245 (5)	6.9 (3)*
C64	−0.3813 (6)	0.1084 (4)	0.2075 (5)	7.1 (3)*
C65	−0.3468 (7)	0.1281 (5)	0.1658 (6)	8.0 (3)*
C66	−0.3022 (6)	0.0950 (4)	0.1349 (5)	6.7 (2)*
C71	−0.2298 (5)	−0.0346 (4)	0.3704 (4)	4.6 (2)
C72	−0.3034 (6)	−0.0389 (4)	0.3801 (5)	6.7 (2)*
C73	−0.3344 (7)	0.0063 (5)	0.4068 (6)	8.0 (3)*
C74	−0.2888 (7)	0.0496 (5)	0.4231 (6)	9.0 (3)*
C75	−0.2163 (8)	0.0549 (5)	0.4126 (6)	9.1 (3)*
C76	−0.1854 (6)	0.0099 (4)	0.3861 (5)	7.2 (3)*
C81	−0.1314 (5)	−0.1248 (3)	0.4188 (4)	4.7 (2)
C82	−0.1688 (6)	−0.1638 (4)	0.4433 (5)	6.7 (2)*
C83	−0.1249 (7)	−0.1900 (5)	0.5049 (6)	8.8 (3)*
C84	−0.0444 (7)	−0.1765 (5)	0.5379 (6)	8.6 (3)*
C85	−0.0070 (6)	−0.1375 (4)	0.5155 (5)	7.4 (3)*
C86	−0.0536 (5)	−0.1107 (4)	0.4533 (5)	5.8 (2)*
C91	−0.1718 (5)	−0.2160 (3)	0.1184 (4)	4.9 (2)
C92	−0.2483 (6)	−0.2005 (4)	0.1143 (5)	6.1 (2)*
C93	−0.3175 (7)	−0.2309 (5)	0.0711 (6)	7.8 (3)*
C94	−0.3056 (7)	−0.2724 (5)	0.0370 (6)	8.3 (3)*
C95	−0.2315 (7)	−0.2882 (5)	0.0425 (6)	9.1 (3)*
C96	−0.1608 (6)	−0.2594 (5)	0.0818 (5)	7.7 (3)*
C101	−0.0426 (5)	−0.2182 (3)	0.2481 (4)	4.7 (2)
C102	−0.0795 (5)	−0.2161 (4)	0.2979 (5)	5.8 (2)*
C103	−0.0450 (6)	−0.2440 (4)	0.3591 (5)	6.8 (2)*
C104	0.0209 (6)	−0.2748 (4)	0.3691 (5)	7.0 (3)*
C105	0.0547 (7)	−0.2792 (5)	0.3201 (6)	7.9 (3)*
C106	0.0233 (6)	−0.2500 (4)	0.2571 (5)	6.9 (2)*
C111	0.660 (1)	0.2650 (7)	0.7909 (8)	13.4 (5)*
C112	0.714 (1)	0.2287 (7)	0.7752 (9)	14.2 (6)*
C113	0.7961 (9)	0.2348 (6)	0.8181 (7)	11.7 (4)*
C114	0.832 (1)	0.2682 (7)	0.8682 (9)	14.1 (6)*
C115	0.776 (1)	0.3072 (8)	0.881 (1)	16.0 (6)*
C116	0.695 (1)	0.2994 (7)	0.8431 (8)	13.1 (5)*
C121	0.467 (1)	0.1117 (7)	0.9133 (8)	12.6 (5)*
C122	0.460 (1)	0.1228 (7)	0.8469 (8)	13.1 (5)*
C123	0.5122 (9)	0.1616 (6)	0.8359 (8)	12.0 (5)*
C124	0.566 (1)	0.1847 (7)	0.8955 (9)	13.7 (5)*
C125	0.5665 (9)	0.1708 (7)	0.9610 (8)	11.9 (4)*
C126	0.5157 (9)	0.1326 (6)	0.9658 (7)	11.5 (4)*
C131	0.505 (1)	0.1233 (9)	0.634 (1)	19.2 (8)*
C132	0.576 (1)	0.1301 (9)	0.611 (1)	18.9 (8)*
C133	0.581 (1)	0.182 (1)	0.583 (1)	19.2 (8)*
C134	0.511 (2)	0.208 (1)	0.557 (1)	22 (1)*
C135	0.456 (2)	0.198 (1)	0.591 (2)	30 (1)*
C136	0.448 (1)	0.158 (1)	0.624 (1)	19.9 (9)*
C141	0.432 (1)	0.0598 (7)	0.282 (1)	14.5 (6)*
C142	0.465 (1)	0.1025 (8)	0.3192 (9)	15.2 (6)*
C143	0.488 (1)	0.1113 (9)	0.388 (1)	18.5 (8)*
C144	0.468 (1)	0.0700 (8)	0.4254 (9)	15.7 (6)*
C145	0.430 (1)	0.0249 (8)	0.3898 (9)	15.0 (6)*
C146	0.412 (1)	0.0217 (7)	0.3208 (9)	14.4 (6)*

[a] Numbers in parentheses are estimated standard deviations. [b] Atoms are labeled to agree with Figure 1. [c] Equivalent isotropic thermal parameters are calculated as $^4/_3[a^2\beta_{11} + b^2\beta_{22} + c^2\beta_{33} + ab(\cos\gamma)\beta_{12} + ac(\cos\beta)\beta_{13} + bc(\cos\alpha)\beta_{23}]$. Values marked by asterisks indicate atoms refined isotropically. [d] Half-occupancy.

solvent for **1** and **3**, they are stable in air.

Discussion

Synthetic Aspects and NMR Behavior. Since the extended cluster **1** resulted from the reaction of n-butylstannoic acid with diphenylthiophosphinic acid, it is presumed that partial oxidation of the thio acid occurred at some point in the reaction process. The amount of oxidation was not large, as **1** was obtained in only a 3% yield. The reaction expressing this behavior is given in eq 1. Thus far, **1** incorporates the highest ratio of phosphinate ligand to stannoic acid for any organooxtin cluster structurally characterized, $2^1/_2$:1.[1b]

$$4\,n\text{-BuSn(O)OH} + 6Ph_2PO_2H + 4Ph_2P(S)OH + 8C_6H_6 \rightarrow [(n\text{-BuSn})_4(OH)_2(O_2PPh_2)_6(S(O)PPh_2)_4]\cdot 8C_6H_6 + 6H_2O \tag{1}$$

Analysis showed that the major product had the composition $[n\text{-BuSn(O)SOPPh}_2]_n$, which could be either a cube ($n = 4$) or a drum ($n = 6$) structure. However, the ^{119}Sn chemical shift of −465 ppm is in the range found for other organotin cubes, −466.1 ± 4.7 ppm,[1b] rather than the range for drum formulations involving phosphorus acids, −487.9 ± 1.8 ppm.[1b] Another component, indicated by a signal in the ^{119}Sn NMR pattern at −544.0 ppm, was not characterized further.

The ease of loss of solvent molecules on exposure of the extended cluster **1** to air was indicated by a weight loss noted over a period of time. Its analysis corresponded to the removal of six of the eight benzene molecules of crystallization. Heating at 70 °C in vacuum for 3 h failed to remove any additional solvent. However, the basic structure exhibited in the solid state appears to be retained in solution. The ^{119}Sn NMR spectrum shows two

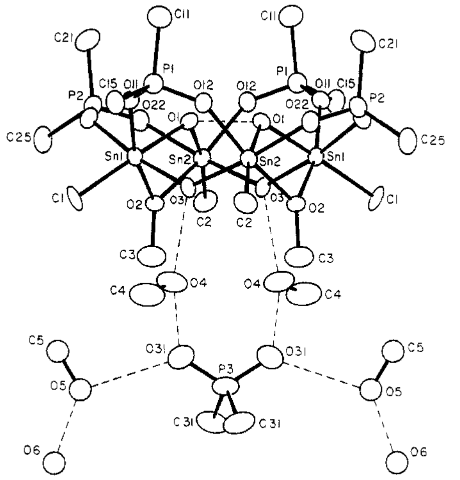

Figure 5. ORTEP plot of $[(MeSn(O)O_2P(t\text{-}Bu)_2)(MeSn(OH)(OMe)O_2P(t\text{-}Bu)_2)]_2[H][O_2P(t\text{-}Bu)_2]\cdot 4MeOH\cdot 2H_2O$ (**3**) with thermal ellipsoids at the 30% probability level. Pendant carbon atoms of the butyl groups are omitted for purposes of clarity. Hydrogen bonding interactions are indicated by dashed lines. Pendant carbon atoms are labeled following the type of scheme given in the caption of Figure 3. Atoms with the same labels are related by a crystallographic 2-fold axis ($-x$, y, $^1/_2 - z$). Atoms C5, O5, and O6 are represented by spheres of arbitrary radius.

multiplets of approximately equal intensities expected for the tetranuclear cluster structure found in the solid state.

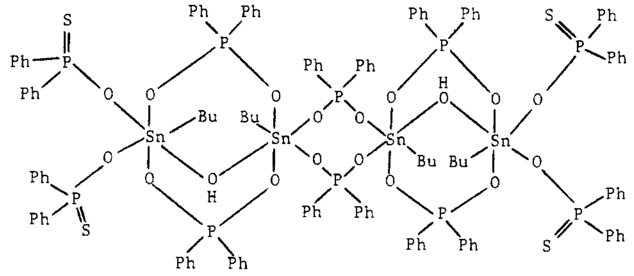

The two signals, at −575.0 and −614.0 ppm, are in the region for hexacoordinated tin. They appear at higher field than that found for other phosphorus-containing butyltin clusters, consistent with the presence of a higher ratio of phosphorus ligand to tin in **1**.[1b] The ^{31}P NMR pattern shows four types of phosphorus atoms, two multiplets in the 20–30 ppm region, assigned to the two types of phosphinate ligands, and two multiplets in the 60–80 ppm region, assigned to the two pairs of thiophosphinate ligands shown in the X-ray structure.

The tetranuclear clusters, **2** and **3**, represent a unique form of tin that have a common skeletal arrangement.

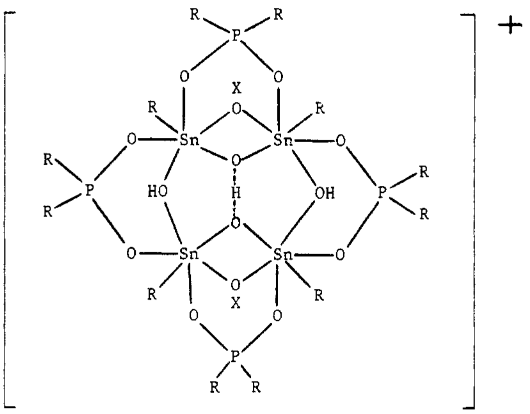

2: R′ = *n*-Bu, R = *t*-Bu, X = H
3: R′ = Me, R = *t*-Bu, X = Me

The butyltin cluster **2** was formed in several reaction schemes. These involved a condensation of the stannoic and phosphinic acids (eq 2), a reaction of *n*-butyltin trichloride with the silver salt of the phosphinic acid (eq 3), and the displacement reaction of the acetate drum, $[n\text{-}BuSn(O)O_2CMe]_6$, with the phosphinic acid (eq 4). The methyltin cluster was obtained simply from the mixed-drum derivative, $[(MeSn(O)O_2CMe)(MeSn(O)O_2P(t\text{-}Bu)_2)]_3$ in a displacement reaction with the phosphinic acid (eq 5). Relative

Table II. Selected Distances (Å) and Angles (deg) for $[(n\text{-}BuSn)_2OH(O_2PPh_2)_3(OSPPh_2)_2]_2\cdot 8C_6H_6$ (**1**)[a]

Distances			
Sn1–O1	2.058 (5)	Sn2–C5	2.16 (1)
Sn1–O11′	2.101 (5)	S4–P4	1.934 (3)
Sn1–O12	2.114 (5)	S5–P5	1.962 (4)
Sn1–O22	2.090 (5)	O4–P4	1.544 (7)
Sn1–O31	2.120 (5)	O5–P5	1.536 (6)
Sn1–C1	2.130 (9)	O11–P1	1.509 (6)
Sn2–O1	2.192 (5)	O12–P1	1.513 (5)
Sn2–O4	2.045 (6)	O21–P2	1.523 (6)
Sn2–O5	2.068 (5)	O22–P2	1.519 (6)
Sn2–O21	2.127 (5)	O31–P3	1.519 (6)
Sn2–O32	2.040 (4)	O32–P3	1.520 (5)

Angles			
O1–Sn1–O11′	84.3 (2)	O4–Sn2–O5	94.0 (2)
O1–Sn1–O12	82.1 (2)	O4–Sn2–O21	85.7 (2)
O1–Sn1–O22	85.9 (2)	O4–Sn2–O32	88.8 (2)
O1–Sn1–O31	83.8 (2)	O4–Sn2–C5	99.7 (3)
O1–Sn1–C1	177.8 (3)	O5–Sn2–O21	164.6 (2)
O11′–Sn1–O12	89.4 (2)	O5–Sn2–O32	81.5 (2)
O11′–Sn1–O22	87.4 (2)	O5–Sn2–C5	98.5 (3)
O11′–Sn1–O31	167.8 (2)	O21–Sn2–O32	83.1 (2)
O11′–Sn1–C1	93.4 (3)	O21–Sn2–C5	96.7 (3)
O12–Sn1–O22	167.8 (2)	O32–Sn2–C5	171.5 (4)
O12–Sn1–O31	91.6 (2)	Sn1–O1–Sn2	135.1 (3)
O12–Sn1–C1	98.1 (3)	Sn2–O4–P4	150.0 (3)
O22–Sn1–O31	89.0 (2)	Sn2–O5–P5	138.7 (3)
O22–Sn1–C1	93.9 (3)	Sn1–O11′–P1′	151.1 (3)
O31–Sn1–C1	98.4 (3)	Sn1–O12–P1	139.1 (3)
O1–Sn2–O4	170.0 (2)	Sn2–O21–P2	133.6 (4)
O1–Sn2–O5	90.7 (2)	Sn1–O22–P2	136.2 (4)
O1–Sn2–O21	87.3 (2)	Sn1–O31–P3	139.5 (3)
O1–Sn2–O32	83.2 (2)	Sn2–O32–P3	136.0 (3)
O1–Sn2–C5	88.3 (3)		

[a] Estimated standard deviations in parentheses. The atom-labeling scheme is shown in Figure 1.

$$4\,n\text{-}BuSn(O)OH + 5(t\text{-}Bu)_2PO_2H \rightarrow [(n\text{-}BuSn(O)O_2P(t\text{-}Bu)_2)(n\text{-}BuSn(OH)_2O_2P(t\text{-}Bu)_2)]_2[H][O_2P(t\text{-}Bu)_2]\ (\text{crown } \mathbf{2}) + 2H_2O \tag{2}$$

$$4\,n\text{-}BuSnCl_3 + 12Ag^+(t\text{-}Bu)_2PO_2^- + 6H_2O \rightarrow [(n\text{-}BuSn(O)O_2P(t\text{-}Bu)_2)(n\text{-}BuSn(OH)_2O_2P(t\text{-}Bu)_2)]_2[H][O_2P(t\text{-}Bu)_2](\text{crown } \mathbf{2}) + 12AgCl + 7(t\text{-}Bu)_2PO_2H \tag{3}$$

$$\tfrac{2}{3}[n\text{-}BuSn(O)O_2CMe]_6 + 5(t\text{-}Bu)_2PO_2H + 2H_2O \rightarrow [(n\text{-}BuSn(O)O_2P(t\text{-}Bu)_2)(n\text{-}BuSn(OH)_2O_2P(t\text{-}Bu)_2)]_2[H][O_2P(t\text{-}Bu)_2](\text{crown } \mathbf{2}) + 4MeCO_2H \tag{4}$$

$$2[(MeSn(O)O_2CMe)(MeSn(O)O_2P(t\text{-}Bu)_2)]_3 + 9(t\text{-}Bu)_2PO_2H + 6MeOH + 6H_2O \rightarrow 3[(MeSn(O)O_2P(t\text{-}Bu)_2)(MeSn(OH)(OMe)O_2P(t\text{-}Bu)_2)]_2[H][O_2P(t\text{-}Bu)_2]\cdot 4MeOH\cdot 2H_2O(\text{crown } \mathbf{3}) + 6MeCO_2H \tag{5}$$

to the synthesis of **2** described in the Experimental Section, eq 2 corresponds to the main preparative route and also to that in Reaction Scheme A, eq 3 describes the synthetic route in Reaction Scheme B, and eq 4 describes the synthesis in Reaction Scheme C.

The complex course of the reactions yielding **2** is illustrated by the ^{119}Sn NMR spectra in Figure 7a–d. Figure 7a shows five products formed after heating the stannoic and phosphinic acid components for 1 h via Reaction Scheme A. The cube derivative,

Table III. Atomic Coordinates in Crystalline $[(n\text{-BuSn(O)O}_2\text{P}(t\text{-Bu})_2)(n\text{-BuSn(OH)}_2\text{O}_2\text{P}(t\text{-Bu})_2)]_2[\text{H}][\text{O}_2\text{P}(t\text{-Bu})_2]$ (**2**)[a]

atom[b]	x	y	z	B_{eq}[c]	atom[b]	x	y	z	B_{eq}[c]
Sn1	0.37079 (6)	0.15867 (3)	0.67283 (3)	3.62 (2)	C31	0.573 (1)	0.1946 (6)	0.4618 (5)	6.6 (4)
Sn2	0.58526 (6)	0.21329 (3)	0.63813 (3)	3.90 (2)	C32	0.467 (1)	0.1694 (6)	0.4720 (5)	6.4 (3)*
Sn3	0.40891 (6)	0.32401 (3)	0.55714 (3)	3.90 (2)	C33	0.661 (1)	0.1487 (7)	0.4669 (6)	7.8 (4)*
Sn4	0.19721 (6)	0.27042 (3)	0.59181 (3)	3.53 (2)	C34	0.559 (1)	0.2222 (8)	0.4074 (7)	9.5 (5)*
P1	0.1447 (2)	0.1307 (1)	0.5880 (1)	4.19 (7)	C35	0.7216 (9)	0.2915 (6)	0.5067 (5)	6.6 (4)
P2	0.5803 (3)	0.0763 (1)	0.6630 (1)	4.66 (7)	C36	0.747 (1)	0.3252 (7)	0.5555 (6)	8.2 (4)*
P3	0.6048 (3)	0.2477 (2)	0.5125 (1)	4.92 (8)	C37	0.822 (1)	0.2572 (7)	0.4960 (7)	8.7 (4)*
P4	0.1775 (3)	0.3389 (1)	0.4794 (1)	4.48 (7)	C38	0.692 (1)	0.3327 (8)	0.4596 (7)	9.4 (5)*
P5	0.4401 (3)	0.3279 (1)	0.7595 (1)	5.10 (8)	C41	0.120 (1)	0.4095 (5)	0.4764 (5)	6.2 (4)
O1	0.4403 (5)	0.1789 (3)	0.6087 (2)	3.4 (2)	C42	0.163 (1)	0.4385 (7)	0.5274 (7)	8.6 (4)*
O2	0.5091 (5)	0.2028 (3)	0.7035 (3)	3.8 (2)	C43	−0.007 (1)	0.4050 (7)	0.4732 (6)	7.9 (4)*
O3	0.3251 (5)	0.2522 (3)	0.5565 (3)	3.6 (2)	C44	0.152 (1)	0.4420 (7)	0.4294 (7)	9.2 (5)*
O4	0.2923 (6)	0.3440 (3)	0.6061 (3)	3.9 (2)	C45	0.149 (1)	0.3002 (6)	0.4193 (5)	5.6 (3)
O5	0.2823 (5)	0.2334 (3)	0.6609 (3)	3.8 (2)	C46	0.178 (1)	0.2423 (7)	0.4337 (7)	9.0 (5)*
O6	0.5121 (6)	0.2921 (3)	0.6235 (3)	4.0 (2)	C47	0.230 (2)	0.3202 (8)	0.3816 (7)	10.3 (5)*
O11	0.2466 (6)	0.1181 (3)	0.6247 (3)	4.5 (2)	C48	0.034 (1)	0.3044 (7)	0.3921 (7)	9.4 (5)*
O12	0.1319 (6)	0.1916 (3)	0.5720 (3)	4.5 (2)	C51	0.540 (1)	0.3864 (6)	0.7679 (5)	7.7 (4)
O21	0.4652 (6)	0.0857 (3)	0.6718 (3)	4.5 (2)	C52	0.481 (1)	0.4424 (7)	0.7545 (7)	8.8 (4)*
O22	0.6366 (6)	0.1287 (3)	0.6473 (6)	4.5 (2)	C53	0.621 (1)	0.3725 (7)	0.7320 (6)	8.1 (4)*
O31	0.5099 (6)	0.2868 (3)	0.5091 (3)	4.9 (2)	C54	0.595 (2)	0.3916 (8)	0.8220 (8)	10.4 (5)*
O32	0.6291 (6)	0.2162 (3)	0.5635 (3)	4.9 (2)	C55	0.328 (1)	0.3369 (6)	0.7960 (5)	7.3 (4)
O41	0.2976 (6)	0.3459 (3)	0.4910 (3)	4.6 (2)	C56	0.373 (2)	0.3456 (8)	0.8568 (8)	10.6 (5)*
O42	0.1280 (6)	0.3070 (3)	0.5203 (3)	4.3 (2)	C57	0.265 (1)	0.2812 (7)	0.7906 (7)	9.1 (5)*
O51	0.3926 (7)	0.3278 (3)	0.7030 (3)	5.3 (2)	C58	0.257 (2)	0.3851 (9)	0.7770 (8)	11.4 (6)*
O52	0.4991 (7)	0.2761 (3)	0.7773 (3)	5.9 (2)	C101	0.323 (1)	0.1375 (5)	0.7457 (5)	5.4 (3)
C11	0.154 (1)	0.0892 (5)	0.5297 (5)	5.6 (3)	C102	0.304 (1)	0.0755 (6)	0.7537 (6)	6.7 (3)*
C12	0.250 (1)	0.1154 (6)	0.5070 (5)	6.0 (3)*	C103	0.276 (2)	0.075 (1)	0.816 (1)	18 (1)*
C13	0.184 (1)	0.0280 (6)	0.5424 (6)	7.4 (4)*	C104	0.282 (4)	0.039 (2)	0.826 (2)	32 (2)*
C14	0.050 (1)	0.0947 (7)	0.4902 (7)	9.3 (5)*	C201	0.738 (1)	0.2437 (6)	0.6729 (5)	6.0 (3)
C15	0.0305 (9)	0.1127 (5)	0.6210 (5)	5.2 (3)	C202	0.767 (1)	0.2257 (7)	0.7297 (6)	8.0 (4)*
C16	0.026 (1)	0.0501 (6)	0.6315 (6)	7.1 (4)*	C203	0.886 (2)	0.254 (1)	0.749 (1)	14.8 (8)*
C17	−0.076 (1)	0.1334 (7)	0.5895 (6)	8.0 (4)*	C204	0.936 (3)	0.220 (1)	0.782 (1)	23 (1)*
C18	0.046 (1)	0.1440 (7)	0.6742 (6)	7.4 (4)*	C301	0.485 (1)	0.4025 (5)	0.5534 (6)	6.6 (4)
C21	0.656 (1)	0.0525 (5)	0.7245 (5)	5.8 (3)	C302	0.472 (2)	0.4427 (9)	0.5939 (8)	12.5 (7)*
C22	0.628 (1)	0.0917 (6)	0.7674 (6)	7.0 (4)*	C303	0.544 (2)	0.4986 (9)	0.5864 (9)	12.9 (7)*
C23	0.780 (1)	0.0547 (6)	0.7205 (6)	7.6 (4)*	C304	0.530 (3)	0.535 (2)	0.617 (1)	24 (1)*
C24	0.627 (1)	−0.0088 (7)	0.7377 (7)	9.0 (5)*	C401	0.064 (1)	0.2962 (5)	0.6286 (5)	5.3 (3)
C25	0.574 (1)	0.0256 (6)	0.6096 (5)	6.6 (4)	C402	0.053 (2)	0.3535 (9)	0.6315 (8)	11.6 (6)*
C26	0.527 (1)	0.0591 (7)	0.5612 (6)	7.7 (4)*	C403	−0.033 (2)	0.3726 (9)	0.6693 (8)	11.6 (6)*
C27	0.689 (1)	0.0064 (7)	0.6011 (7)	9.0 (5)*	C404	−0.067 (2)	0.426 (1)	0.646 (1)	19 (1)*
C28	0.501 (2)	−0.0244 (8)	0.6181 (8)	10.7 (6)*					

[a] Numbers in parentheses are estimated standard deviations. [b] Atoms are labeled to agree with Figure 3. [c] Equivalent isotropic thermal parameters are calculated as $^4/_3[a^2\beta_{11} + b^2\beta_{22} + c^2\beta_{33} + ab(\cos\gamma)\beta_{12} + ac(\cos\beta)\beta_{13} + bc(\cos\alpha)\beta_{23}]$. Values marked with asterisks indicate atoms refined isotropically.

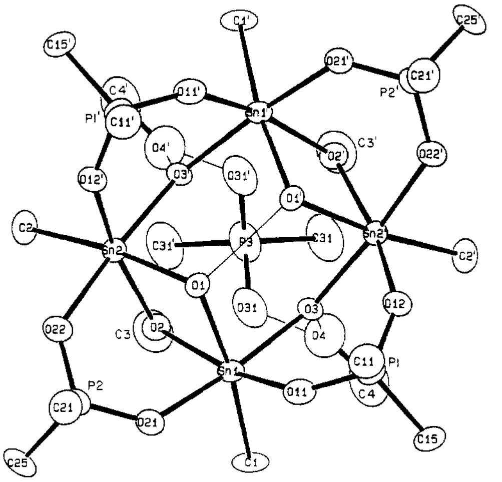

Figure 6. ORTEP plot of **3** viewed down the crystallographic 2-fold axis with thermal ellipsoids at the 30% probability level. Pendant carbon atoms of the butyl groups and the loosely bound MeOH and H_2O molecules are omitted for purposes of clarity. Primed atoms are 2-fold related to unprimed ones ($-x, y, {}^1/_2 - z$). Hydrogen-bonding interactions are shown as narrow solid lines.

$[n\text{-BuSn(O)O}_2\text{P}(t\text{-Bu})_2]_4$, previously characterized by X-ray analysis and NMR,[1b] shows its presence by the low-field triplet at −474.9 ppm (^2J(Sn–O–P) = 128 Hz). The remainder of the spectra, Figure 7b–d, other than the insert on (d), are obtained at successive stages of separation as described in the main preparation leading to the pure crown cluster **2**. Hence, the doublet of doublets centered at −535.3 ppm corresponds to **2**. A similar pattern is present at −525.5 ppm with ^2J(Sn–O–P) coupling constants of 139 and 204 Hz. This suggests the presence of a related cluster derivative, possibly the neutral crown species, $[(n\text{-BuSn(O)O}_2\text{P}(t\text{-Bu})_2)(n\text{-BuSn(OH)}_2\text{O}_2\text{P}(t\text{-Bu})_2)]_2$, which could form by loss of a molecule of phosphinic acid. However, we were unable to verify the latter suggestion. The compounds giving rise to the triplet patterns at −513 ppm (^2J(Sn–O–P) = 151 Hz) and at −530.5 ppm (^2J(Sn–O–P) = 143 Hz) are not identified, although the former triplet might arise from the presence of an oxygen-capped cluster, i.e., $[(n\text{-BuSn(OH)O}_2\text{P}(t\text{-Bu})_2)_3\text{O}][\text{O}_2\text{P}(t\text{-Bu})_2]$. The range of chemical shifts on known O-capped derivatives is −498 to −509 ppm,[1b] extending to near the value observed here. However, the suggested O-capped substance has not been independently synthesized.

A similar ^{119}Sn NMR spectrum resulted from the reaction of $n\text{-BuSnCl}_3$ with the silver salt of the phosphinic acid (Reaction Scheme B, eq 3) showing the presence of all the components discussed for the reaction of eq 1, except that the triplet at −530.5 ppm was absent.

In Reaction Scheme C, eq 4, in addition to the crown cluster **2**, a symmetric mixed-drum derivative, $[(n\text{-BuSn(O)O}_2\text{CMe})(n\text{-BuSn(O)O}_2\text{P}(t\text{-Bu})_2)]_3$, was indicated by the presence of a doublet pattern in the ^{119}Sn spectrum at −491.2 ppm (^2J(Sn–O–P) = 132 Hz). The range formed for phosphorus acid containing drum compounds covers the ^{119}Sn chemical shift region from −486 to −493 ppm.[1b,8]

Table IV. Selected Distances (Å) and Angles (deg) for $[(n\text{-BuSn(O)O}_2\text{P}(t\text{-Bu})_2)(n\text{-BuSn(OH)}_2\text{O}_2\text{P}(t\text{-Bu})_2)]_2[\text{H}][\text{O}_2\text{P}(t\text{-Bu})_2]$ (**2**)[a]

	Distances		
Sn1–O1	2.062 (7)	Sn3–C301	2.14 (1)
Sn1–O2	2.110 (7)	Sn4–O3	2.023 (7)
Sn1–O5	2.122 (7)	Sn4–O4	2.148 (7)
Sn1–O11	2.114 (7)	Sn4–O5	2.168 (6)
Sn1–O21	2.131 (7)	Sn4–O12	2.110 (7)
Sn1–C101	2.15 (1)	Sn4–O42	2.146 (7)
Sn2–O1	2.063 (6)	Sn4–C401	2.15 (1)
Sn2–O2	2.098 (7)	O11–P1	1.527 (7)
Sn2–O6	2.127 (7)	O12–P1	1.531 (8)
Sn2–O22	2.146 (7)	O21–P2	1.522 (8)
Sn2–O32	2.110 (8)	O22–P2	1.536 (8)
Sn2–C201	2.15 (1)	O31–P3	1.521 (8)
Sn3–O3	2.031 (7)	O32–P3	1.531 (8)
Sn3–O4	2.142 (7)	O41–P4	1.518 (8)
Sn3–O6	2.166 (7)	O42–P4	1.524 (8)
Sn3–O31	2.116 (8)	O51–P5	1.520 (8)
Sn3–O41	2.143 (7)	O52–P5	1.497 (9)
O1–O3	2.565 (9)	O2–O52	2.64 (1)
O5–O51	2.82 (1)	O6–O51	2.88 (1)
O4–O51	2.71 (1)		
	Angles		
O1–Sn1–O2	76.5 (3)	O4–Sn3–O41	90.0 (3)
O1–Sn1–O5	87.4 (3)	O4–Sn3–C301	100.5 (4)
O1–Sn1–O11	89.4 (3)	O6–Sn3–O31	88.9 (3)
O1–Sn1–O21	83.1 (3)	O6–Sn3–O41	173.1 (3)
O1–Sn1–C101	171.2 (4)	O6–Sn3–C301	97.2 (4)
O2–Sn1–O5	91.2 (3)	O31–Sn3–O41	90.3 (3)
O2–Sn1–O11	165.9 (3)	O31–Sn3–C301	91.9 (5)
O2–Sn1–O21	89.1 (3)	O41–Sn3–C301	89.7 (4)
O2–Sn1–C101	95.8 (4)	O3–Sn4–O4	78.2 (3)
O5–Sn1–O11	88.4 (3)	O3–Sn4–O5	87.6 (3)
O5–Sn1–O21	170.2 (3)	O3–Sn4–O12	90.1 (3)
O5–Sn1–C101	97.2 (4)	O3–Sn4–O42	86.8 (3)
O11–Sn1–O21	89.0 (3)	O3–Sn4–C401	175.7 (4)
O11–Sn1–C101	98.3 (4)	O4–Sn4–O5	89.7 (3)
O21–Sn1–C101	92.4 (4)	O4–Sn4–O12	168.1 (3)
O1–Sn2–O2	76.7 (3)	O4–Sn4–O42	87.9 (3)
O1–Sn2–O6	87.2 (3)	O4–Sn4–C401	97.9 (4)
O1–Sn2–O22	84.2 (3)	O5–Sn4–O12	88.1 (3)
O1–Sn2–O32	90.1 (3)	O5–Sn4–O42	174.2 (3)
O1–Sn2–C201	175.5 (4)	O5–Sn4–C401	94.2 (4)
O2–Sn2–O6	91.0 (3)	O12–Sn4–O42	93.3 (3)
O2–Sn2–O22	87.7 (3)	O12–Sn4–C401	93.9 (4)
O2–Sn2–O32	166.9 (3)	O42–Sn4–C401	91.3 (4)
O2–Sn2–C201	100.6 (4)	Sn1–O1–Sn2	104.4 (3)
O6–Sn2–O22	171.3 (3)	Sn1–O2–Sn2	101.5 (3)
O6–Sn2–O32	88.1 (3)	Sn3–O3–Sn4	105.1 (3)
O6–Sn2–C201	96.6 (4)	Sn3–O4–Sn4	97.3 (3)
O22–Sn2–O32	91.2 (3)	Sn1–O5–Sn4	131.6 (3)
O22–Sn2–C201	92.1 (4)	Sn2–O6–Sn3	131.4 (3)
O32–Sn2–C201	92.5 (4)	Sn1–O11–P1	141.0 (5)
O3–Sn3–O4	78.1 (3)	Sn4–O12–P1	140.7 (4)
O3–Sn3–O6	87.7 (3)	Sn1–O21–P2	132.5 (4)
O3–Sn3–O31	89.5 (3)	Sn2–O22–P2	131.9 (5)
O3–Sn3–O41	85.4 (3)	Sn3–O31–P3	140.1 (5)
O3–Sn3–C301	174.6 (4)	Sn2–O32–P3	141.4 (5)
O4–Sn3–O6	89.3 (3)	Sn3–O41–P4	131.4 (5)
O4–Sn3–O31	167.5 (3)	Sn4–O42–P4	131.7 (4)

[a] Estimated standard deviations in parentheses. The atom-labeling scheme is shown in Figure 3.

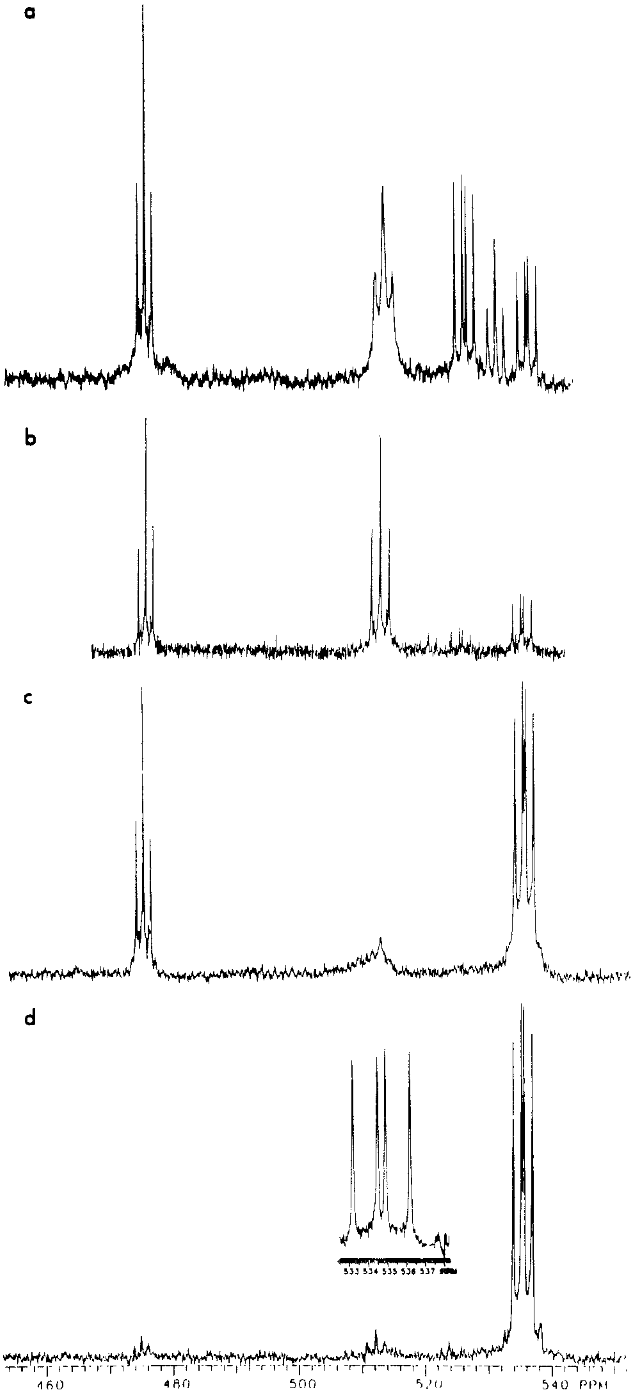

Figure 7. ^{119}Sn NMR spectra of the crown cluster **2** obtained (a) after 1 h of heating a 1:1.25 mole ratio mixture of *n*-BuSn(O)OH and $(t\text{-Bu})_2PO_2H$ in a 1:1 methanol/toluene solvent system (Reaction Scheme A), (b) from a recrystallization from a benzene/methylene chloride/ether mixture after reaction of a 1:2 mole ratio of *n*-BuSn(O)OH and $(t\text{-Bu})_2PO_2H$ (main preparation), (c) from the same reaction as in (b) but after a further crystallization using a methanol/chloroform/ether solvent mixture, and (d) from the same reaction as in (b) but on the final product. The inset shows an enlarged spectrum of a pure sample of **2** resulting from Reaction Scheme C. All spectra are in $CDCl_3$ solution except (b) where C_6D_6 was used.

Examination of ^{31}P NMR spectra obtained on the same samples that were used to construct the ^{119}Sn NMR spectra for Figure 7, showed an entirely analogous interpretation. For example, the ^{31}P NMR signals (in $CDCl_3$) and assignments for the sample used to obtain the ^{119}Sn spectrum in Figure 7c are the cube formulation at 64.6 ppm (^2J(Sn–O–P) = 124 Hz) and the crown **2** at 58.6 ppm. Figure 8a shows the ^{31}P NMR spectrum of a pure sample of **2** in $CDCl_3$ solution resulting from Reaction Scheme C, eq 4. At this resolution, the near accidental degeneracy of the signals due to the two different pairs of phosphorus atoms in the cluster of **2** is apparent. The signal for the $(t\text{-Bu})_2PO_2^-$ anion is located upfield at 50.7 ppm. Details of the tin satellite pattern caused by ^2J coupling with phosphorus are shown in an expanded pattern of the main signal in Figure 8b.

The preparation of the analogous crown cluster **3** from the mixed-drum derivative, eq 5, results in a relatively high yield, 70%, compared to a 20% yield for **2**. Just prior to the final crystallization, residual mixed-drum reactant, **5**, is detected in the ^{119}Sn NMR spectrum by the doublet at −471.0 ppm, Figure 9a. Also a triplet at −452.9 ppm, ^2J(Sn–O–P) = 118.5 Hz, is indicative of a cube formulation, most likely of composition [MeSn-

Table V. Atomic Coordinates in Crystalline $[(MeSn(O)O_2P(t\text{-}Bu)_2)(MeSn(OH)(OMe)O_2P(t\text{-}Bu)_2)][H][O_2P(t\text{-}Bu)_2]\cdot 4MeOH\cdot 2H_2O$ (3)[c]

atom[b]	x	y	z	B_{eq}[c]	atom[b]	x	y	z	B_{eq}[c]
Sn1	0.01184 (4)	0.07065 (5)	0.14672 (3)	3.10 (2)	C16	−0.1855 (8)	0.0653 (9)	0.0958 (6)	7.2 (4)
Sn2	0.12450 (4)	0.06798 (5)	0.24193 (3)	3.05 (2)	C17	−0.2486 (7)	0.203 (1)	0.1024 (6)	8.2 (5)
P1	−0.1220 (2)	0.1952 (2)	0.1479 (1)	3.95 (7)	C18	−0.1508 (8)	0.183 (1)	0.0368 (5)	7.6 (5)
P2	0.1588 (2)	0.1560 (2)	0.1203 (1)	3.99 (8)	C21	0.1690 (7)	0.2663 (8)	0.1159 (5)	5.4 (3)
P3	0.000[d]	−0.3180 (3)	0.250[d]	5.6 (1)	C22	0.239 (1)	0.293 (1)	0.138 (1)	13.1 (7)
O1	0.0446 (3)	0.1306 (4)	0.2148 (3)	2.9 (2)	C23	0.162 (1)	0.300 (1)	0.0571 (6)	8.8 (5)
O2	0.0837 (4)	−0.0087 (4)	0.1808 (3)	3.3 (2)	C24	0.1140 (9)	0.3008 (9)	0.1532 (7)	8.7 (5)
O3	−0.0633 (3)	0.0192 (5)	0.1969 (3)	3.2 (2)	C25	0.2121 (7)	0.0981 (9)	0.0708 (5)	5.6 (3)
O11	−0.0541 (4)	0.1660 (4)	0.1309 (3)	4.0 (2)	C26	0.1987 (9)	0.0088 (8)	0.0822 (6)	8.3 (4)
O12	−0.1462 (4)	0.1628 (5)	0.2022 (3)	3.8 (2)	C27	0.2847 (8)	0.115 (2)	0.0833 (8)	12.8 (7)
O21	0.0881 (4)	0.1358 (5)	0.1049 (3)	3.8 (2)	C28	0.1904 (9)	0.116 (1)	0.0122 (5)	8.2 (5)
O22	0.1775 (4)	0.1307 (5)	0.1782 (3)	4.1 (2)	C31	−0.0763 (8)	−0.3801 (9)	0.2540 (7)	7.8 (5)
O31	−0.0054 (5)	−0.2684 (6)	0.1975 (4)	6.6 (3)	C32	−0.1316 (7)	−0.315 (1)	0.2711 (7)	8.1 (5)
C1	−0.0081 (7)	0.0003 (8)	0.0738 (5)	5.0 (3)	C33	−0.0933 (9)	−0.416 (1)	0.1972 (8)	9.9 (5)
C2	0.2105 (6)	−0.0058 (8)	0.2590 (5)	4.6 (3)	C34	−0.0733 (9)	−0.448 (1)	0.2973 (8)	9.1 (5)
C3	0.0865 (9)	−0.0984 (9)	0.1777 (7)	7.2 (4)	O4	−0.0775 (5)	−0.1409 (6)	0.1760 (4)	7.4 (3)
C11	−0.1174 (7)	0.3066 (8)	0.1559 (5)	5.7 (4)	C4	−0.1202 (9)	−0.162 (1)	0.1406 (8)	9.1 (5)
C12	−0.0599 (7)	0.3203 (8)	0.2013 (6)	5.5 (4)	O5	0.009 (1)	−0.324 (2)	0.083 (1)	30 (1)*
C13	−0.093 (1)	0.3490 (9)	0.1019 (7)	9.8 (6)	C5	0.026 (2)	−0.259 (3)	0.059 (2)	29 (2)*
C14	−0.1792 (7)	0.3428 (9)	0.1818 (7)	7.7 (5)	O6	−0.089 (2)	−0.448 (2)	0.037 (2)	32 (2)*
C15	−0.1789 (6)	0.1634 (8)	0.0947 (5)	4.6 (3)					

[a] Numbers in parentheses are estimated standard deviations. [b] Atoms are labeled to agree with Figure 5. [c] Equivalent isotropic thermal parameters are calculated as $^4/_3[a^2\beta_{11} + b^2\beta_{22} + c^2\beta_{33} + ab(\cos\gamma)\beta_{12} + ac(\cos\beta)\beta_{13} + bc(\cos\alpha)\beta_{23}]$. Values marked with asterisks indicate atoms refined isotropically. [d] Fixed.

Table VI. Selected Distances (Å) and Angles (deg) for $[(MeSn(O)O_2P(t\text{-}Bu)_2)(MeSn(OH)(OMe)O_2P(t\text{-}Bu)_2)]_2[H][O_2P(t\text{-}Bu)_2]\cdot 4MeOH\cdot 2H_2O$ (3)[a]

Distances			
Sn1–O1	2.037 (7)	Sn2–O22	2.148 (7)
Sn1–O2	2.122 (7)	Sn2–C2	2.16 (1)
Sn1–O3	2.127 (7)	O2–C3	1.47 (2)
Sn1–O11	2.093 (8)	O11–P1	1.515 (9)
Sn1–O21	2.136 (8)	O12–P1	1.506 (8)
Sn1–C1	2.15 (1)	O21–P2	1.517 (8)
Sn2–O1	2.028 (7)	O22–P2	1.517 (8)
Sn2–O2	2.116 (7)	O31–P3	1.52 (1)
Sn2–O3′	2.096 (7)	O4–O3	2.69 (1)
Sn2–O12′	2.112 (7)	O4–O31	2.60 (1)
O1–O1′	2.49 (1)	O5–O31	2.95 (4)
		O5–O6	3.06 (1)
Angles			
O1–Sn1–O2	75.8 (3)	O2–Sn2–O3′	92.3 (3)
O1–Sn1–O3	87.6 (3)	O2–Sn2–O12	166.3 (3)
O1–Sn1–O11	89.8 (3)	O2–Sn2–O22	88.5 (3)
O1–Sn1–O21	84.8 (3)	O2–Sn2–C2	96.7 (4)
O1–Sn1–C1	171.5 (4)	O3′–Sn2–O12′	87.0 (3)
O2–Sn1–O3	91.4 (3)	O3′–Sn2–O22	172.3 (3)
O2–Sn1–O11	165.6 (3)	O3′–Sn2–C2	97.3 (4)
O2–Sn1–O21	89.7 (3)	O12′–Sn2–O22	90.4 (3)
O2–Sn1–C1	97.0 (4)	O12′–Sn2–C2	96.9 (4)
O3–Sn1–O11	86.8 (3)	C22–Sn2–C2	90.2 (4)
O3–Sn1–O21	171.8 (3)	Sn1–O1–Sn2	106.3 (3)
O3–Sn1–C1	97.2 (4)	Sn1–O2–Sn2	100.3 (3)
O11–Sn1–O21	90.1 (3)	Sn1–O2–C3	128.2 (8)
O11–Sn1–C1	97.4 (4)	Sn2–O2–C3	127.9 (8)
O21–Sn1–C1	90.7 (4)	Sn1–O3–Sn2′	132.8 (4)
O1–Sn2–O2	76.1 (3)	Sn1–O11–P1	140.1 (5)
O1–Sn2–O3′	87.2 (3)	Sn2′–O12–P1	139.2 (5)
O1–Sn2–O12′	90.2 (3)	Sn1–O21–P2	132.5 (4)
O1–Sn2–O22	85.6 (3)	Sn2–O22–P	132.5 (5)
O1–Sn2–C2	171.7 (4)		

[a] Estimated standard deviations in parentheses. The atom-labeling scheme is shown in Figure 5.

$(O)O_2P(t\text{-}Bu)_2]_4$.[22] The crown, **3**, appears upfield as a doublet-of-doublets at −512.8 ppm in this spectrum, although the ^{119}Sn resonance for the isolated pure product is observed at a slightly higher field, −515.4 ppm, ^2J(Sn–O–P) = 139 and 181 Hz. A low-field shoulder to **3**, which appears at −509.6 ppm in Figure 9a, is shifted to −511.5 ppm, J = 124, 170 Hz, in an expansion of the crown region, Figure 9b. The latter was obtained at an earlier stage in the crystallization process (see the Experimental Section). The low-field signal may be indicative of a related crown formed by loss of solvent or, as with **2**, a neutral entity formed by loss of a molecule of phosphinic acid.

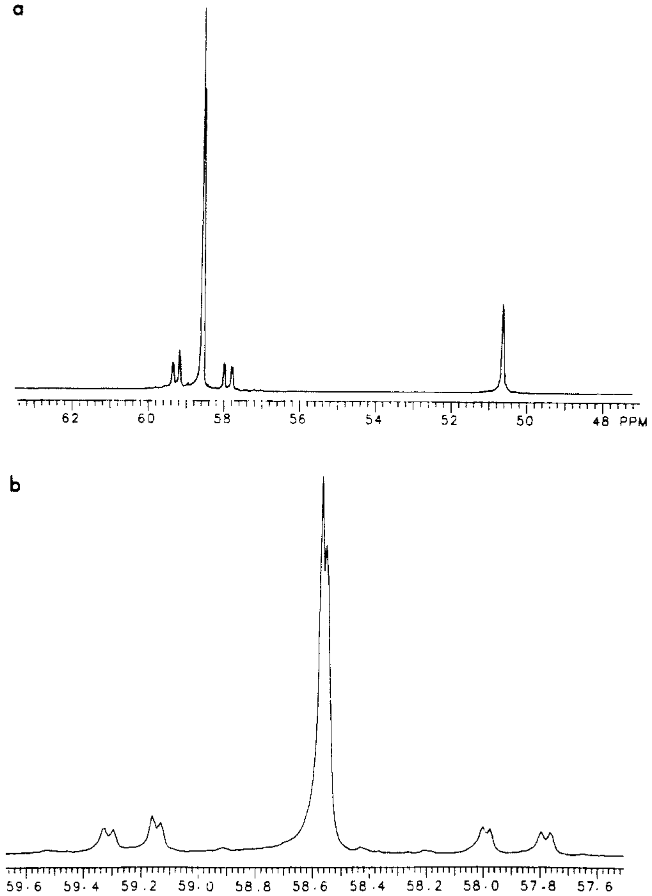

Figure 8. (a) ^{31}P NMR spectrum of a pure sample of the crown cluster **2** in $CDCl_3$ solution resulting from Reaction Scheme C. The corresponding ^{119}Sn NMR spectrum is shown as an inset in Figure 7d. (b) Expansion of the main ^{31}P signal showing two resonances for **2** at 58.56 and 58.54 ppm with tin satellite coupling.

In contrast to **2**, which showed near degeneracy of the expected two ^{31}P signals for the cluster unit, the ^{31}P NMR spectrum of **3**,

---

[22] Nadim, H.; Day, R. O.; Holmes, R. R., unpublished work.

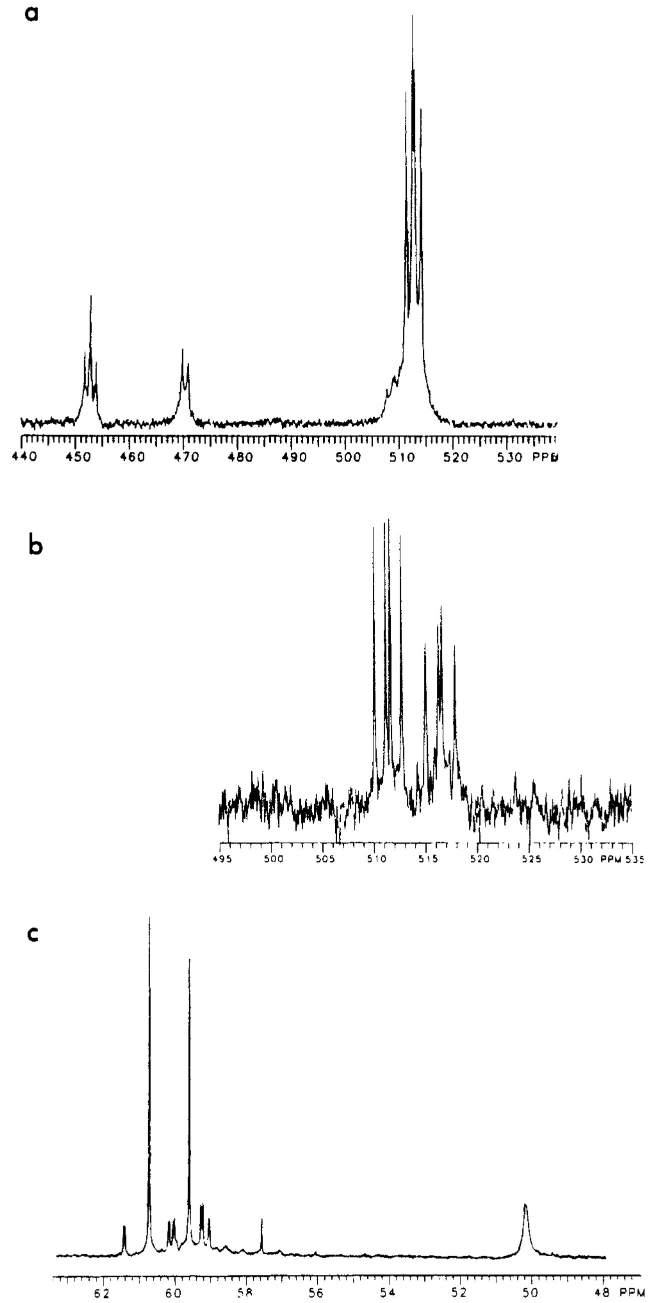

Figure 9. (a) ^{119}Sn NMR spectrum of the crown cluster **3** at an intermediate stage prior to the final crystallization. (b) ^{119}Sn NMR spectrum of the crystalline material obtained from the reaction mixture shown in Figure 9a prior to the isolation of pure crown **3** showing an expansion of the crown cluster region, and (c) ^{31}P NMR spectrum of **3**. All spectra are obtained in $CDCl_3$/MeOH solvent mixture.

Figure 9c, shows well-separated singlets, 60.7 and 59.6 ppm, with similar tin satellite coupling as in the ^{31}P spectrum for **2**. The signal for the anionic phosphinate appears at 50.2 ppm, a somewhat broadened singlet. The broadening is likely due to exchange of the phosphinate between hydrogen bonding sites involving methanol and water molecules, Figure 5.

The adoption of both tetranuclear clusters, **2** and **3**, in the skeletal arrangement of form A, shown in the introduction, rather than in the adamantyl framework is consistent with the tendency of monoorganooxotin clusters to maintain a hexacoordinate, octahedral environment around tin and to form four-membered stannoxane rings.[1-10] The only organooxotin oligomer obtained so far that is an exception is found in the structure of the highly phosphinated cluster, **1**. It is also the only cluster prepared so far that has thiophosphinate ligands. The latter have a greater tendency than phosphinates to act as monodentate rather than bidentate groups. As detailed in the following section, this tetranuclear cluster contains six-membered and eight-membered ring units involving phosphinate ligands and Sn–O(H)–Sn units, Figures 1 and 2, respectively.

The existence of a structure that contains the $(Sn-O)_2$ ring system with hexacoordinated tin and exhibits both Sn–S and Sn–O bonding with mercaptoethanolate ligands, B,[23] suggests that cluster

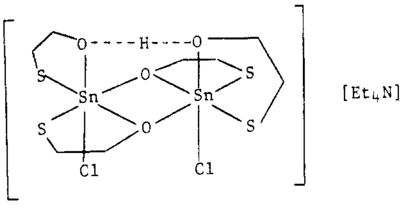

B

units related to **1**–**3** are possible that might possess both P–O–Sn and P–S–Sn bonding. Further, it would be interesting to study related systems containing Sn–S–Sn bonding in competition with Sn–O–Sn bonding. So far the $(Sn-S)_2$ ring has remained elusive.[24]

Detailed Structural Analysis. All three compounds contain four tin centers and have dimeric formulations. **1** is an opened dimer, while **2** and **3** are cyclic dimers. The tin atoms are in all cases hexacoordinated, bonded to one carbon atom and five oxygen atoms, and have octahedral coordination geometry. The phosphinate ligands form symmetrical bridges between tin atoms in all cases, while the thiophosphinate ligands, present only in **1**, are dangling (vide infra). In compounds **2** and **3** there is also a free phosphinate group present as a counterion in the lattice.

For all three compounds, electrical neutrality demands the inclusion of protons in the frameworks. Since the positions of the hydrogen atoms could not be obtained from the X-ray data, these positions have been inferred from the non-hydrogen atom geometry (vide infra).

Compound **1** has a crystallographic inversion center, which relates the halves of the dimer, Figure 2. The idealized molecular symmetry is also C_i. There are therefore two types of tin atoms in the molecule. Electrical neutrality demands the inclusion of two protons in the framework of the molecule. The logical placement for these protons is either on the bridging oxygen atom, O1, or on the dangling sulfur atoms, S4 or S5, Figure 1. The P–S bond lengths, 1.934 (3) and 1.962 (4) Å, are typical of P=S double bonds,[25] and therefore it is concluded that the O1 atoms represent bridging hydroxyl groups.

The six phosphinate groups in the molecule form symmetrical bridges between adjacent tin atoms. These bridges fall into two categories. The two symmetry-related phosphinate groups containing P1 bridge the symmetry-related Sn1 atoms, which are not otherwise connected, to form an eight-membered $(Sn-O-P-O)_2$ ring about a crystallographic inversion center. The remaining four phosphinate groups form pairs of bridges between pairs of tin atoms (Sn1 and Sn2), which are also connected by hydroxyl bridges. The four thiophosphinate groups, two bonded to each terminal tin atom through the oxygen atom, appear to be dangling. The three closest intramolecular Sn–S distances (Sn2–S5 = 4.131 (3) Å, Sn2–S4 = 4.300 (3) Å, Sn1–S5 = 5.224 (3) Å) are too long to suggest any sort of bonding interaction. While S5 is so disposed as to suggest a hydrogen bonding interaction to the bridging hydroxyl group, O1, the distance S5–O1 = 3.549 (6) Å is larger than the van der Waals sum of 3.30 Å,[26] and if such an interaction obtains, it is probably a weak one.

With regard to the types of chemically distinct phosphorus atoms in **1**, there are three. Two of the type forming the central

---

(23) Holmes, R. R.; Shafieezad, S.; Chandrasekhar, V.; Holmes, J. M.; Day, R. O. *J. Am. Chem. Soc.* **1988**, *110*, 1174–1180.

(24) Note added in proof. We now have synthesized $[(n\text{-BuSn}(S)O_2PPh)_3O]_2Sn$. It is a double cube containing both $(Sn-S)_2$ and (–Sn–O–Sn–Sn–) rings: Kumara Swamy, K. C.; Day, R. O.; Holmes, R. R., submitted for publication.

(25) Huheey, J. E. *Inorganic Chemistry*, 3rd ed.; Harper & Row: New York, 1983.

(26) Bondi, A. *J. Phys. Chem.* **1964**, *68*, 441–456.

eight-membered ring (P1 and P1′), four of the type that bridge tin atoms that are also bridged by hydroxyl group (P2, P3, P2′, and P3′), and four of the type found in the dangling thiophosphinate groups.

Of the three structures, **1** is unique in that it contains the eight-membered phosphorus-containing ring and is missing the four-membered $(Sn{-}O)_2$ ring, which prevails in related compounds.[1-10] It is interesting to note that, if the hydroxyl bridge (O1) between Sn1 and Sn2 were absent, an eight-membered $(Sn{-}O{-}P{-}O)_2$ ring would result.

Compound **2** has no crystallographic symmetry. However, the idealized molecular symmetry of the framework is C_{2v}. This symmetry can be seen easily in Figure 4 where the view is down the pseudo 2-fold axis. One vertical mirror plane passes ideally through O1, O2, O3, O4, and phosphorus atoms P2 and P4 while the other, perpendicular to the first, contains O5, O6, P1, and P3. There are, therefore, four chemically equivalent tin atoms and two pairs of chemically distinct phosphorus atoms in the framework.

For compound **2**, electrical neutrality demands the inclusion of five protons in the Sn, O, and P framework. The unusually close proximity of O1 and O3 (2.565 (9) Å), Figure 3, and their apparent chemical equivalence strongly suggest the presence of a symmetrical hydrogen bond of the sort that we have reported recently in related structures.[23,27] The remaining four protons can be assigned to the remaining four bridging oxygen atoms O2, O4, O5, and O6, or three of them can be placed there with the fourth associated with the free phosphinate group. Since the four aforementioned bridging oxygen atoms ideally occur in symmetry-related pairs, it seems reasonable to view the four of them, each with an associated proton, as bridging hydroxyl groups. The molecular structure of compound **3** argues in favor of this viewpoint (vide infra). Thus, the tin cluster with a proton associated with O1 and O_3 is viewed as a cationic species, with the anionic phosphinate group present as a counterion. The proximity of the oxygen atoms of the free phosphinate group to the bridging hydroxyl groups suggests fairly strong, hydrogen bonding interactions[28] (O2–O52 = 2.64 (1) Å, O4–O51 = 2.71 (1) Å), Figure 3.

The chemically equivalent phosphinate groups in **2** containing P1 and P3 bridge tin atoms that are also bridged by hydroxyl groups, while the remaining pair containing P2 and P4 form diagonal bridges across the faces of the four-membered $(Sn{-}O)_2$ rings. The former structural motif is also found in compound **1**, while the latter is present in the drum,[8] the cube,[1b,9] the oxygen-capped cluster,[10] and the butterfly[1b] structures. The four tin atoms together with the bridging hydroxyl groups form an eight-membered $(Sn{-}O)_4$ ring in the shape of an elongated crown. This is a structural motif that has not previously been observed in related compounds.

In compound **3**, which has crystallographic C_2 symmetry, the framework of the stannoxane dimer is the same as that in compound **2**, but with methyl groups in place of the *n*-butyl groups and with two of the bridging hydroxyl groups replaced by bridging methoxy groups, Figure 6. Like **2**, the idealized symmetry of the framework is C_{2v}, and there is one type of tin and two types of phosphorus present.

The difference between **2** and **3** in the solid state is caused primarily by the solvent present in the lattice of **3**. In **2**, the free phosphinate group is hydrogen bonded directly to the hydroxyl groups of the tin moiety. In **3**, two symmetry-related methanol molecules are sandwiched between the phosphinate groups and the tin moiety, apparently as a result of hydrogen bonding interactions, Figure 5. In addition, there are two more loosely bound methanol molecules as well as two water molecules per cyclic dimer. Three protons are required to maintain electrical neutrality and their placement can be made with more confidence here. Since the free phosphinate group has crystallographic C_2 symmetry, the equivalence of its P–O bonds precludes the placement of one of the protons on this moiety. Two of the protons are thus assigned to the symmetry-related bridging hydroxyl groups O3 and O3′, while the third is placed between the symmetry-related O1 and O1′, which are in very close proximity (O1–O1′ = 2.49 (1) Å).

The hydrogen bonding in the lattice, as inferred from the non-hydrogen atom geometry, is in agreement with the placement of the three protons (Figure 5): The hydroxyl oxygen atom O3 acts as a proton donor to oxygen atom O4 of the methanol molecule, which, in turn, acts as a proton donor to O31 of the phosphinate group. Atom O5 of a second methanol molecule acts as a second proton donor to atom O31 and in turn accepts a proton from the water oxygen atom O6. The pertinent oxygen–oxygen distances are O3–O4 = 2.69 (1) Å, O4–O31 = 2.60 (1) Å, O5–O31 = 2.95 (4) Å, and O5–O6 = 3.06 (1) Å.

It is interesting to view the tin moieties in compounds **2** and **3** as inherently neutral molecules that have become cationic species by the abstraction of a proton from a phosphinic acid molecule.

Acknowledgment. The support of this research by the National Science Foundation, Grant CHE-8504737, and the donors of the Petroleum Research Fund, administered by the American Chemical Society, is gratefully acknowledged.

Registry No. 1, 116184-76-0; **1**·$8C_6H_6$, 116184-77-1; **2**, 116184-82-8; **3**, 116184-84-0; **3**·$4MeOH{\cdot}2H_2O$, 116261-24-6; **4**, 116184-79-3; $Ph_2P(S)OH$, 14278-72-9; *n*-$BuSn(O)O_2CCH_3)$, 80685-38-7; diphenylchlorophosphine, 1079-66-9; *n*-butylstannoic acid, 2273-43-0; di-*tert*-butylphosphinic acid, 677-76-9; *n*-butyltin trichloride, 1118-46-3; silver di-*tert*-butylphosphinate, 116184-78-2.

Supplementary Material Available: Thermal parameters and additional bond lengths and angles (Tables S1–S2, respectively, for **1**, Tables S3—S4 for **2**, and Tables S5–S6 for **3**) (22 pages); tables of observed and calculated structure factor amplitudes for **1–3** (77 pages). Ordering information is given on any current masthead page.

---

[27] Holmes, R. R.; Shafieezad, S.; Chandrasekhar, V.; Sau, A. C.; Holmes, J. M.; Day, R. O. *J. Am. Chem. Soc.* **1988**, *110*, 1168–1174.

[28] Pimental, G. C.; McClellan, A. L. *The Hydrogen Bond*; Freeman: San Francisco, CA, 1960.